International Journal of Engineering& Scientific Research
Vol.12 Issue 06, June 2024
ISSN: 2347-6532 Impact Factor: 8.076
Journal Homepage: http://www.ijmra.us, Email: editorijmie@gmail.com
Double-Blind Peer Reviewed Refereed Open Access International Journal - Included in the International Serial Directories Indexed & Listed at: Ulrich's Periodicals Directory ©, U.S.A., Open J-Gage as well as in Cabell's Directories of Publishing Opportunities, U.S.A

Flow and Noise Studies in Supersonic Rectangular Slot Jets

Jeshwanth Kundem[**]

Abstract

Jet noise is a serious problem for aircraft engine designers. Not only in airplanes, every jet flow is accompanied by noise. Of late, non-circular jets are promising candidates for noise reduction. Orifices can be used to study jet flows rather than conventional nozzles to bring out the effect of geometry. The present paper experimentally investigates the variation of pressure and noise in different regions of slot jets. Focus is made on the rectangular slot jets. The shadowgraph method is used to visualize the jet flow. The variation in pressure in a rectangular jet along the major axis is studied concerning noise data and shadowgraph images. The crossing over of OASPL values for rectangular geometry along major and minor axes along the shear layer of the jet is analyzed.

Keywords:
Orifice plate;
Rectangular jets;
Shadowgraph visulaziation;
Anechoic Chamber;

Author correspondence:
Jeshwanth Kundem
Email:
jeshwanth.kundem@outlook.com

1. Introduction

Jet flows are an important part of various mixing devices and thrust-producing systems. Free jets issued out from nozzles/orifices are momentum-driven flows. High-speed free jets are further classified as subsonic, overexpanded, moderately under-expanded, and highly under-expanded jets (Donaldson and Snedeker, 1971) depending upon the nozzle pressure ratio. The jet is considered to be subsonic if the ratio of stagnant pressure to ambient pressure is less than 1.89. This ratio is termed as nozzle pressure ratio. The flow field of jets is classified (Sforza et al., 1966) into three distinct zones: potential core, transition region, and fully developed region. The fluid mass addition takes place in all three zones of jet through entrainment.

Jet flows occur in various situations, and the geometries, sizes, and flow conditions cover a large range. Jet flows vary greatly, depending on the values of two numbers. The first is the Reynolds number, and the second is the Mach number. At low Reynolds numbers (Re < 2000) and M << 1, jet flows take on a simple character. An example is the water jet formed by a household tap when the valve is partially opened to produce a low flow. If the flow diameter increases or the viscosity

[*]* Mechanical Engineering Department, IIT Guwahati, Assam, India (when research was conducted)

decreases to increase the Reynolds number, the jet changes dramatically. For example, a water jet exiting into the water at rest with Re 2300 is unstable and the flow undergoes a transition to a more chaotic turbulent state. The large-scale structures are responsible for capturing fluid from the surroundings and entraining it into the jet. However, the jet and external fluids are not thoroughly mixed until the small-scale structures complete diffusion. Different methods have been investigated to change their entrainment rates to control mixing and thrust. A technique for increasing the entrainment rate is found by using a small aspect ratio elliptic jet (Ho and Gutmark 1987, Hussain and Hussain 1989). Schadow et al. (1987) investigated triangular control of flow coherence.

When the velocities in the jet are greater than the speed of sound (M > 1) the flow is said to be supersonic, and important qualitative changes in the flow occur. The most prominent change is the occurrence of shock waves. These mechanisms like expansion fans and shocks arise to equilibrate the jet pressure with that of the ambient. Such imperfectly expanded jets can be generated using convergent or convergent-divergent nozzles. For example, a supersonic air jet exhausting from a nozzle at low pressure into higher-pressure air at rest is said to be over-expanded. As the jet leaves the nozzle, it senses the higher pressure around it and adjusts through oblique shock waves emanating from the edges of the nozzle. The oblique shock waves are caused due to the reflection of the expansion waves from the jet boundary. The expansion and compression wavefronts combine to form shock cell patterns or shock diamonds. For moderately under expanded conditions, the shock cell patterns are formed until the pressure of the jet flow is equalized with that of the ambient.

Another class of jet flows is identified by the fact that the motion of the jet is induced primarily by buoyancy forces. A common example is a hot gas exhaust rising in the atmosphere. Such jet flows are called buoyant plumes, or simply plumes, as distinct from the momentum jets, or simply jets, discussed above. The jet flows have a wide range of applications like laser jet printing, and propulsion systems. Jet flows are largely used in aircraft to generate thrust for propulsion.

2. Research Method – Flow Visualization

Moving fluids often form patterns so complicated that intuition fails when we try to imagine them. Some flows are so complicated that we cannot analyze all their details from the governing equations, even with the biggest computers now available. Flow visualization is the study of methods to display dynamic behavior in liquids and gases. It is the art of making flow patterns visible.

In time-dependent flows, different flow patterns succeed one another, making it very difficult to obtain an understanding of the flow phenomena from the output of a few probes at fixed locations. Various visual techniques can then be used as experimental tools for determining the general nature of a complicated flow and also to provide quantitative measurements of such things as speed, frequency, density, time sequences, etc.,

Many kinds of flow visualization are known and have been employed in research, development, or teaching. They are grouped into five major types: (i) marker methods, (ii) optical methods, (iii) wall trace methods, (iv) birefringence, and (v) self-visible phenomena.

Shadowgraph is an optical method that reveals non-uniformities in transparent media like air, water, or glass. It is related, but simpler than the Schlieren and Schlieren photography methods that perform a similar function. Schlieren photography is a visual process that is used to photograph the flow of fluids of varying density. The basic optical schlieren system uses light from a single collimated source shining on, or from behind, a target object. Variations in refractive index caused by density gradients in the fluid distort the collimated light beam. The distortion creates a spatial variation in the intensity of the light, which can be visualized directly with a shadowgraph system. The shadowgraph system measures the second derivative of density.

3. Experimental Configuration

Jet Facility

The free test facility is supplied with compressed air from two tanks of capacity 10 m^3 each. The air is pressurized using a 150 HP two-stage, inter-cooled reciprocating air compressor driven by a three-phase induction motor. The compressor is far from the experimental setup. The

compressor can be used to pressurize the air upto an absolute pressure of 8 bar. Figure 1 shows the layout of the test facility. The pressure inside the settling chamber is regulated using a needle valve.

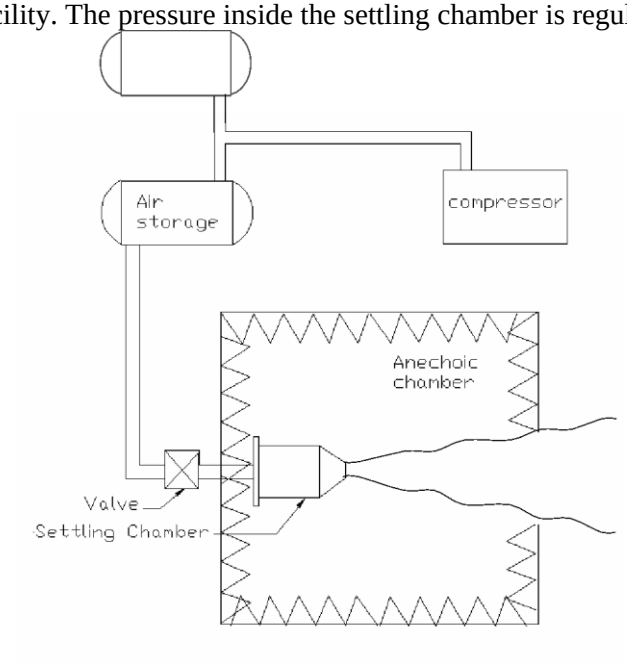

Figure 1: *Layout of the test facility*

The settling chamber has a length of around 700 mm and an internal radius of 190mm. Meshes are provided inside the settling chamber to eliminate internal disturbances such as turbulence. The settling chamber is smoothly converged to the diameter of 43.5 mm where the orifices of the required geometry can be mounted using a disk holder. Acoustic foam is fixed to all reflective surfaces to minimize the reflections.

Anechoic Chamber

An anechoic chamber (an-echoic or non-echoing) is a room designed to stop reflections of either sound or electromagnetic waves. They are also insulated from exterior sources of noise. The combination of both aspects means they simulate a quiet open space of infinite dimension, which is useful when exterior influences would otherwise give false results.

Anechoic chambers are commonly used in acoustics to conduct experiments in nominally "free field" conditions. All sound energy will be traveling away from the source with almost none reflected back. In general, the interior of an anechoic chamber is very quiet, with typical noise levels in the 10–20 dB range. According to Guinness World Records, 2005 (The Quietest Place on Earth – Orfield Labs), Orfield Laboratory's NIST-certified Eckel Industries-designed anechoic chamber is "The quietest place on earth" measured at −9.4 dB. The human ear can typically detect sounds above 0 dB, so a human in such a chamber would perceive the surroundings as devoid of sound. The University of Salford has a number of Anechoic chambers, of which one is unofficially the quietest in the world with a measurement of −12.4 dB.

Full anechoic chambers aim to absorb energy in all directions. Semi-anechoic chambers have a solid floor that acts as a work surface for supporting heavy items, such as cars, washing machines, or industrial machinery, rather than the mesh floor grille over absorbent tiles found in full anechoic chambers. This floor is damped and floating on absorbent buffers to isolate it from outside vibration or electromagnetic signals. A recording studio may utilize a semi-anechoic chamber to produce high-quality music free of outside noise and unwanted echoes.

The air jet facility and the requisite components at IIT Madras are enclosed in a semi-anechoic chamber of dimension 2.5 m x 2 m x 2 m (wedge tip to tip) to simulate a free field environment (Figure 2). Square pyramidal wedges are adhered to the walls of the chamber except the floor which is lined with carpet, and hence the chamber is semi-anechoic. The wedges are made of polyurethane foam material. The chamber is calibrated by verifying inverse square law along various linear paths inside the chamber. The law followed up to the frequency value of 630 Hz

below which the chamber was not anechoic and is therefore the cut-off frequency of the anechoic chamber.

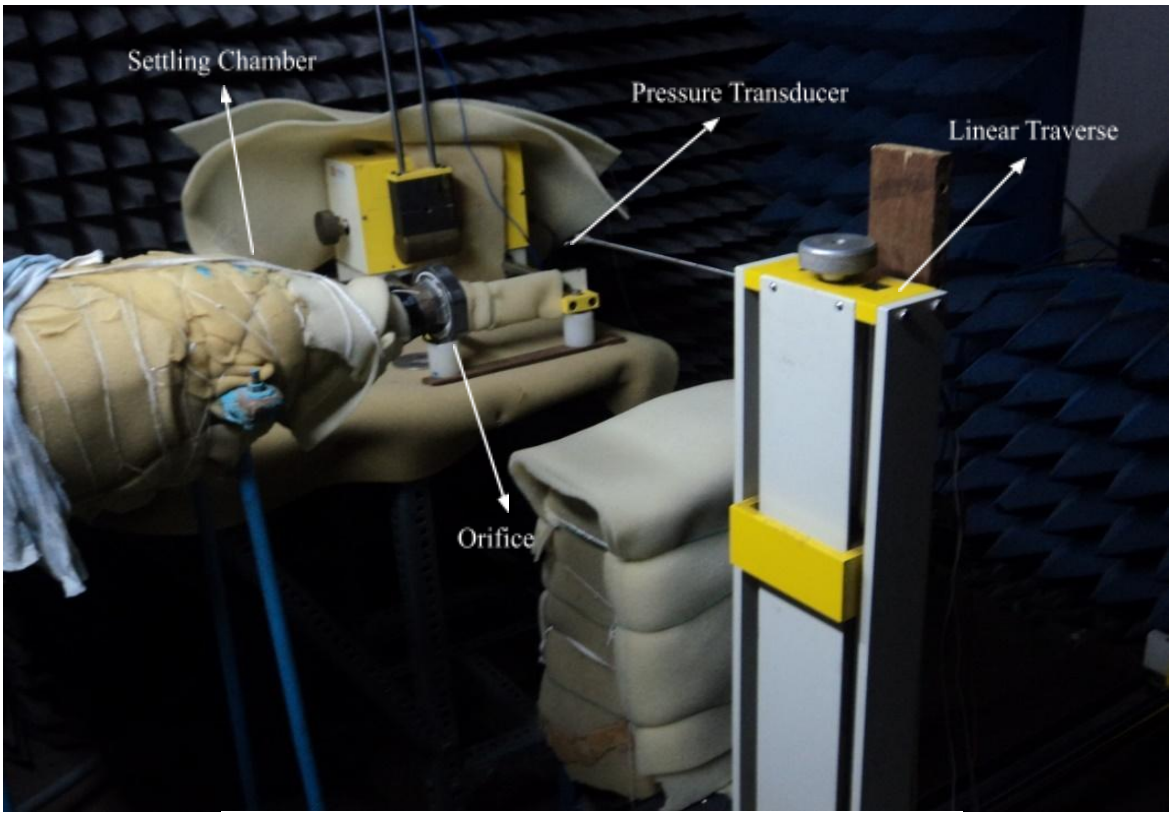

Figure 2: *Photograph of Experimental setup in the anechoic chamber*

Slot Models

The slots or "disk nozzles" (Figure 3) are fabricated using mild steel plate of 73 mm diameter and 2 mm thickness. The required circular and non-circular shapes are cut out at the center of this disk using Electro Discharge Machining (EDM)/wire cutting process. All the non-circular geometries used are designed for a constant exit area of 78.5 mm^2, equivalent to the area of a circle of diameter 10 mm. Thus, the equivalent diameter of non-circular jets is 10 mm.

Using slots instead of conventional nozzles eliminates the azimuthally varying boundary layer effects (Hussain and Hussain, 1989) due to the negligible shear layer thickness in slots. Furthermore, as pointed out by Quinn and Marsters (1985), in some applications, "expeditious manufacturing and ease of installation may necessitate the use of slots in preference to nozzles with contoured upstream shaping".

Figure 3: *Photograph of Circular and Rectangular slots*

Data Acquisition System

Pressure measurements are carried out using Kulite pressure transducer XCQ-093 series, having an input pressure range of 0.35 to 70 bar and a diameter of 2.4 mm.

The sensor is connected to the preamplifiers and signal conditioner. The signal is low-pass filtered at 70 KHz using an analog filter (Krohn-Hite model no.3364) for anti-aliasing as shown in Figure 4. BNC connectors are used for the data transfer. The data are acquired at a sampling rate of 150 KHz for one second using an eight-channel simultaneous sampling card from National Instruments (NI-PCI-6143) (Figure 5). This card has an ADC resolution of 16 bits with a maximum sampling rate of 250 KSa/s.

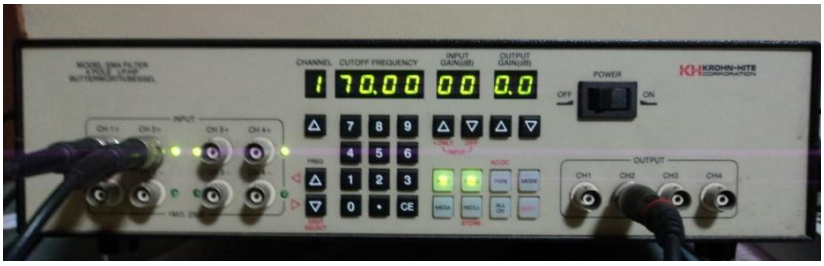

Figure 4: *Analog Filter*

Figure 5: *NI Card*

Linear Traverse

The studies are made using custom custom-designed linear traversing system (Figure 6). The motion of it is synchronized with the data acquisition system and can move along three directions. The stepper motor of the traverse is controlled by a stepper drive (National Instruments NI-MID-7604) and the motion is automated using LabView 7.1 software. The transducer is fixed such that the front portion of it points towards the jet exit.

DC Supply

The pressure transducer required a DC for its performance. So, an Aplab Regulated DC Power supply (Figure 7) is used which has a line voltage of 230V AC, 50 Hz, Single phase, tolerance of 10%, and an operating temperature of 0-50 degrees Centigrade. The least count of it is 0.1Volts. The major problem with DC supply its settling time is very high.

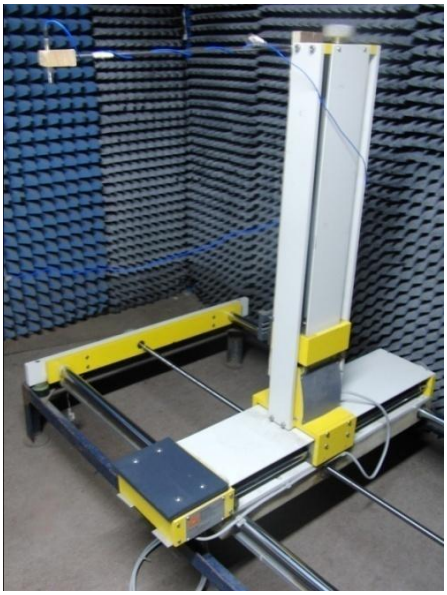

Figure 6: *Photograph of Linear Traverse*

Figure 7: *Photograph of DC Supply*

3. Results & Analysis

The time series data from the kuilite pressure transducer are analyzed using MATLAB 7.2 to obtain the dynamic pressure values. In this section, the pressure variation of circular and rectangular geometries is presented. The temperature inside the anechoic chamber while conducting experiments is 34^{o}C. Experiments are carried out at a nozzle pressure ratio of 3.

The pressure transducer is moved from 10 mm for the geometries with the help of linear traverse operated by Labview software. The readings are taken for every 5 mm of the traverse. The pressure sensor being very small in size it is having more fluctuations. So it is held manually during the experiment so that it won't get out off the center line.

In the initial stages of the experiment both the sound pressure and dynamic pressure readings are taken simultaneously. But the sound pressure readings do not seem to be in the correct pattern. This is due to the reflections of the pressure transducer. Later on the readings are taken individually and correct pattern is observed. Figure 8 shows the pressure variation with an increase in distance from jet. It is compared with the shadow graph image (Figure 9) of the circular jet from previous works.

From figure 8 the maximum value of pressure occurs at an x/d value of 8.0, it shows clear relation with Shadow graph image where the shock cell ends at around 80mm. The maximum dynamics pressure value occurred is 11260 Pascals.

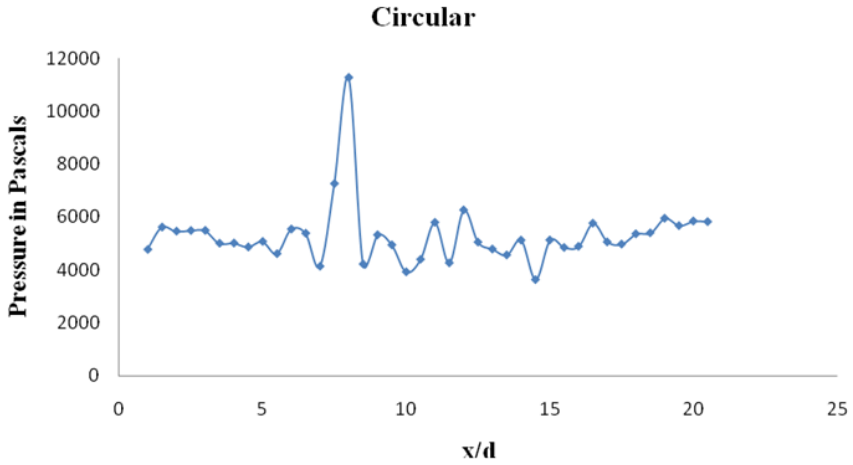

Figure 8: *Pressure variation of a circular jet*

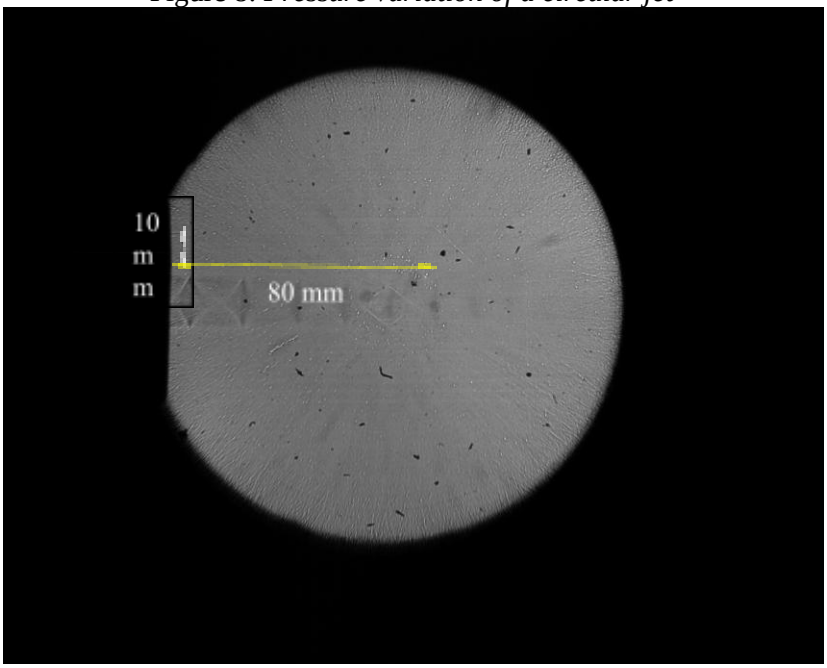

Figure 9: *Shadow graph image of circular slot jet*

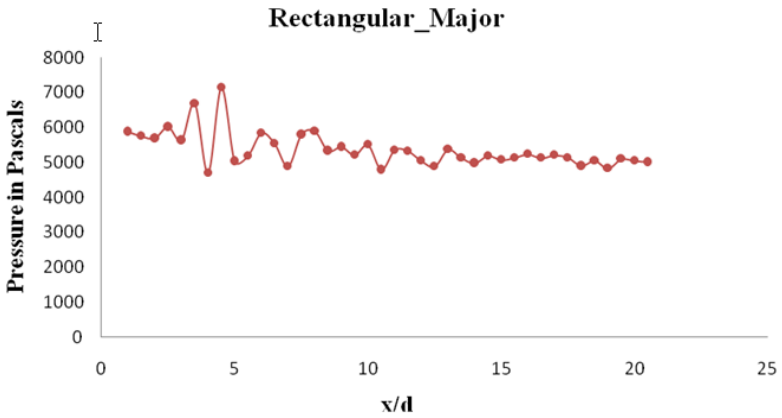

Figure 10: *Dynamic pressure variation for rectangular slot jet*

When the pressure measurements for rectangular geometry of aspect ratio 7:2 are observed, the maximum pressure occurred at an x/d of 4.5 (Figure 10). It shows clear relation with shadow graph images where the shock ends at around 45 mm from the jet exit (Figure 11).

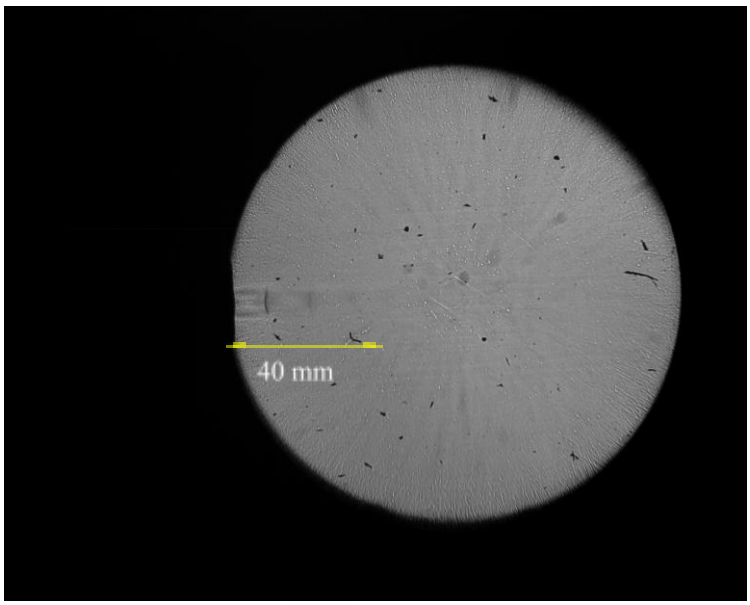

Figure 11: *Shadow graph image for rectangular major*

In Figure 12 the OASPL behavior for rectangular geometry is shown. The maximum value occurs at 40 mm. The sound level decreases after maximum variation at around 40 mm. We can conclude that the maximum pressure is related to the maximum OASPL value and the ending of shock. When the dynamic pressure readings for circular and rectangular are compared, they come up with a passionate variation

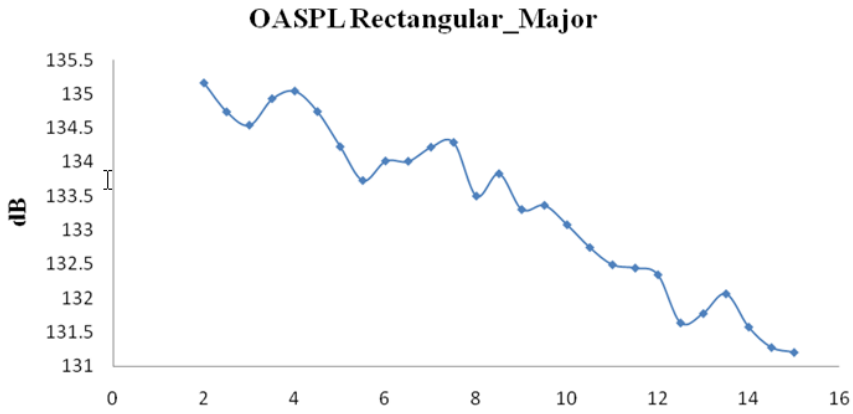

Figure 12: *OASPL for rectangular major*

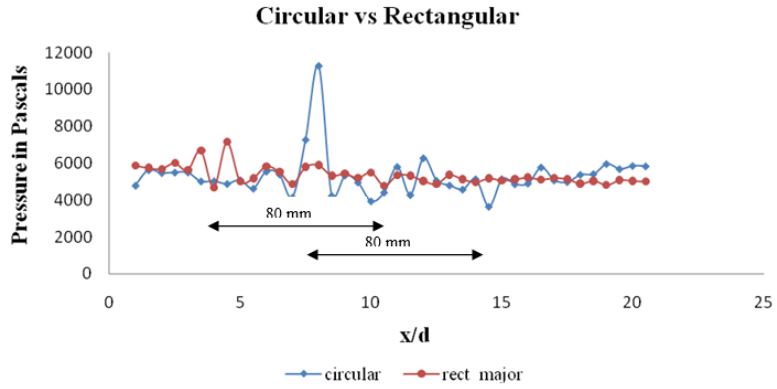

Figure 13: *Comparison of circular & rectangular geometries*

For same distance past the end of the shock, both circular and rectangular geometries exhibited random fluctuation. After some more distance along the jet there is no noticeable fluctuation in the behavior (Figure 13). The fluctuating distance is shown clearly in the figure. The fluctuations for rectangular geometry are less than that of the circular geometry.

More over the maximum value of pressure for Circular geometry is 1.5 times that of the maximum value for rectangular geometry (~7148 pascals). At the end of the shock in circular the variation is in positive side while for rectangular it is on both sides, this may be due to the axis switching of the jet in the rectangular geometry.

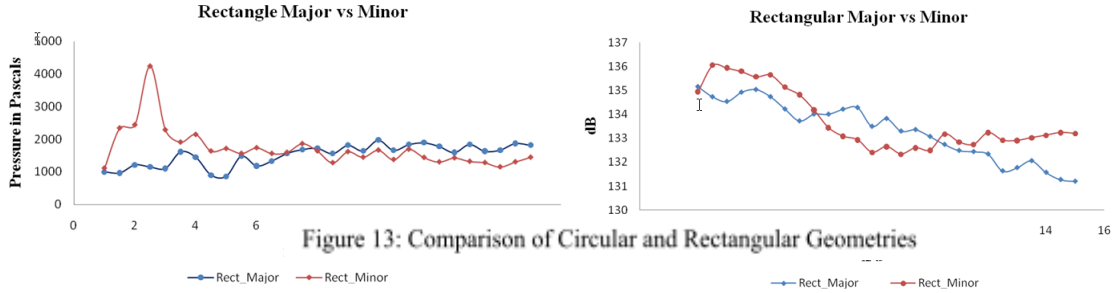

Figure 13: Comparison of Circular and Rectangular Geometries

Figure 14 & 15: *OASPL Variation along shear layer for rectangular along major & minor axis*

The dynamic pressure variation is also observed along the shear layer for rectangular jets in both major and minor axis. The shear layer values are taken by the Pitot tube. The pressure transducer is moved along the shear layer to capture the dynamic pressure values. Figure 14 shows the behavior of pressure along the shear layer for Rectangular jets (major and minor). The pressure values are compared with their OASPL values (Figure 15). The cross over for the jets is observed.

The cross over in the OASPL data in the region of 6 to 10 x/d is due to the variation in dynamic pressure along the layer. The microphone is taking the data at 4D, if we take the readings

at exactly in the shear layer, we can get the cross over at x/d of 8. It might not be due to the axis switching.

The shear layer thickness changes according to the geometry of the jet. The high pressure at the starting of the jet for rectangular minor axis is due to the shock cell structure (Figure 16). For this geometry the shock cell length is more that is the reason why the increament in pressure is more for minor when compared to major. The geometry variation is also one factor for the shock length variation.

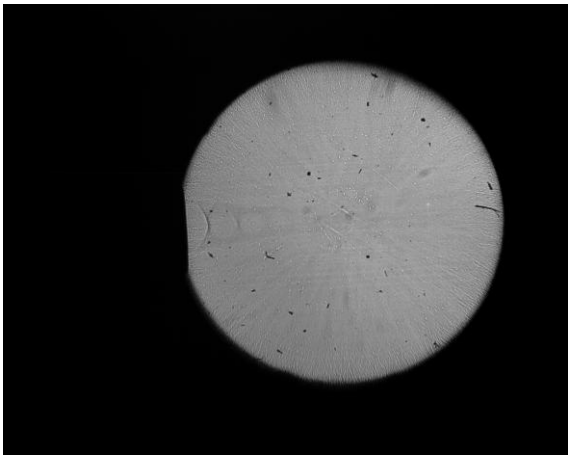

Figure 16: *Shadowgraph image for rectangular along minor axis*

The shock cell structure for rectangular geometry is not strong when compared to that of circular slot jet. It can be the reason why the noise levels are decreasing for rectangular jets when compared to circular. For minor axis the shock cell structure length is more compared to that of the major. This is due to the geometry. For minor it suffices for more distance along the jet, but for major it dissipates soon.

Conclusion

Studies have been conducted to understand & minimize the flow noise in circular and rectangular jets. Anechoic chamber along with various noise measurement instrumentation at various distances from he nozzle were used. Results indicated that with rectangular configuration there is an improvement in noise reduction. The rectangular sizes should be optimized, in further research.

References

[1] T.J.S. Jothi and K.Srinivasan, (2008) Acoustic characteristics of non-circular slot jets, *Acta Acustica United with Acustica*, 92, 229-242

[2] G. N. Abramovich (1963) The Theory of Turbulent Jets, *MIT Press*, Massachusetts Institute of Technology, Cambridge Massachusets.

[3] N. Rajaratnam (1976) Turbulent Jets, *Elsevier Scientific Publishing Company*, University of Alberta, Edmonton, Alberta, Canada.

[4] Christopher K.W. Tam (1995) Supersonic Jet Noise, Florida State University, Tallahassee, Florida 32306-3027.

[5] Ganesh Raman and K Srinivasan, Design Characteristics of Anechoic Chamber

[6] John M.Seiner and James C. Yu (1984) Acoustic Near-field properties Associated with Broadband shock Noise, *AIAA Journal*, Vol. 22, No. 9

[7] Donaldson, C.D. and R.S. Snedeker (1971) Study of Free Jet Impingement. Mean properties of Free and Impinging Jets, *Journal of Fluid Mechanics*, 45, 281-324

[8] Sforza, P.M, M.H. Steiger and N. Trentacoste (1966) Studies on three dimensional viscous jets, *AIAA Journal*, (4), 800-806

[9] Schadow, K.C., E. Gutmark, D.M. Parr, and K. J. Wilson(1988) Selective control of flow coherence in triangular jets, *Experiments in Fluids*, 6, 129-135

[10] Hussain, A.K.M.F. and H.S. Husain (1989) Elliptic jets. Part 1: Characteristics of unexcited and excited jets. *Journal of Fluid Mechanics.* 208, 257-320

[11] Ho, C.M. and E. Gutmark (1987) Vortex induction and mass entrainment in a small aspect ratio elliptic jet. *Journal of Fluid Mechanics*, 110, 39-71

[12] Settles, G.S. (2001). Schlieren and Shadowgraph techniques: Visualizing phenomena in transparent media. Berlin : Springer-Verlag

[13] Russel Merritt and J. B. Kaufman (2006) Walt Disney's Silly Symphonies : A companion to the classis cartoons series, Italy : La Cinecita del Friuil, page 46

[14] Holman, J. Alan (2001) Experimental methods for engineers, Boston: *McGraw-Hill*

[15] Prandtl, L. and Tietjens, O. G., Fundamentals of Hydro and Aero Mechanics, *McGraw-Hill*, 1934, Chapter-V